Cellular Automata and Lattice Boltzmann Techniques: An Approach to Model and Simulate Complex Systems

Bastien Chopard
Computer Science Department
University of Geneva, 1211 Geneva 4, Switzerland

Abstract

We discuss the cellular automata approach and its extensions, the lattice Boltzmann and multiparticle methods. The potential of these techniques is demonstrated in the case of modeling complex systems. In particular, we consider simple applications taken from various scientific domains.

Contents

1 The Cellular Automata approach

1.1 A model of reality

A natural way to describe a physical, chemical or biological system is to propose a model of what we think is happening. During this process we usually retain only the ingredients we believe to be essential in order to capture the behavior we are interested in. Using an appropiate mathematical machinery, such a model can then be expressed in terms a set of equations whose solution gives the desired answers on the system. The description in terms of equations is very powerful and corresponds to a rather high level of abstraction. For a long time, this methodology has been the only tractable way for scientists to address a problem.

Another approach, which has been made possible by the advent of fast computers, is to stay at the level of the model and its basic components. The idea is that all the information is already contained in the model and that a computer simulation will be able to answer any possible question on the system by just running the model for some time. Thus, there is no need to use a complicated mathematical tool to obtain a high level of description. We just need to express the model in a way which is suitable to an effective computer implementation. The cellular automata is a paradigm in which simple models of complex phenomena can be easily formulated. In particular, cellular automata models illustate the fact that a complex behavior emerges out of many simply interacting components through a collective effect.

The degree of reality of the model depends on the level of description we expect. When we are interested in the global or macroscopic properties of a system (and this is the case here) the microscopic details of a system are often irrelevant. On the other hand, symmetries and conservation laws are usually the essential ingredients. It is therefore a clear advantage to invent a much simpler microscopic reality, which is more appropriate to our numerical means of investigation.

A cellular automata model can be seen as a fictitious universe which has its own microscopic reality but, nevertheless, has the same macroscopic behavior as the real system we are interested in. The example we shall give in the next section will illustrate this statement.

1.2 Brief history

Cellular automata (often termed CA) are an idealization of a physical system in which space and time are discrete. In addition, the physical quantities (or state of the automaton) take only a finite set of values. Since it has been invented by von Neumann in the late 1940s, the cellular automata approach has been applied to a large range of scientific problems [1–4]).

The original motivation of von Neumann was to extract the abstract mecha-

nisms leading to self-reproduction of the biological organisms[5]. In other words the problem is to devise a system having the capability (and the recipe) to produce another organism of equivalent complexity with only its own ressource.

Following the suggestions of S. Ulam[6], von Neumann addressed this question in the framework of a fully discrete universe made up of cells. Each cell is characterized by an internal state, which typically consists of a finite number of information bits. Von Neumann suggested that this system of cells evolves, in discrete time steps, like simple automata which only know of a simple recipe to compute their new internal state. The rule, determining the evolution of this system is the same for all cells and is a function of the states of the neighbor cells. Similarly to what happens in any biological system, the activity of the cells takes place simultaneously. However, the same clock drives the evolution of each cell and the updating of the internal state of each cell occurs synchronously.

Such a fully discrete dynamical systems (cellular space) as invented by von Neumann are now referred to as a *cellular automaton.*

After the work of von Neumann, other authors have followed the same line of research and nowadays the problem is still of interest [7] and has lead to interesting developments for new computer architectures [8].

Many other applications of CA's to physical science have been considered. In 1970, the mathematician John Conway proposed his famous *game of life*[9]. His motivation was to find a simple rule leading to complex behaviors. He imagined a two-dimensional square lattice, like a checkerboard, in which each cell can be either alive (state one) or dead (state zero). The updating rule of the game of life is as follows: a dead cell surrounded by exactly three living cells gets back to life; a living cell surrounded by less than two or more than three neighbors dies of isolation or overcrowdness. Here, the surrounding cells corresponds to the neighborhood composed of the four nearest cells (north, south, east and west), plus the four second nearest neighbors, along the diagonals. It turns out that the game of life automaton has an unexpectedly rich behavior. Complex structures emerge out of a primitive "soup" and evolve so as to develop some skills. Figure 1 shows some configurations of the game of life automaton.

As for von Neumann rule, the game of life is a cellular automata capable of universal computations: it is always possible to find an initial configuration of the cellular space reproducing the behavior of any electronic gate and, thus, to mimic any computation process. Although this observation has little practical interest, it is very important from a theoretical point of view since it assesses the ability of CAs to be a non restrictive computational technique.

A very important feature of CAs is that they provide simple models of complex systems. They exemplify the fact that a collective behavior can emerge out of the sum of many, simply interacting, components. Even if the basic and local interactions are perfectly known, it is possible that the global behavior obeys new laws that are not obviously extrapolated from the individual properties, as if the whole is more than the sum of all the parts. This properties makes cellular

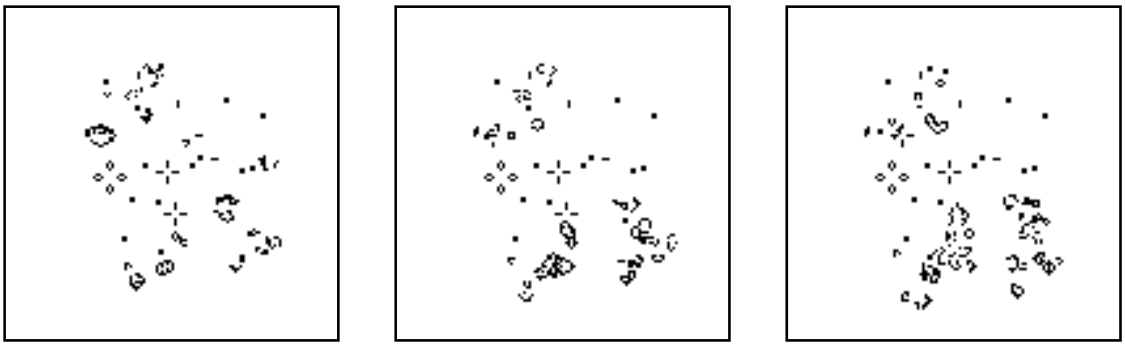

Figure 1: *The game of life automaton. Black dots represents living cells whereas dead cells are white. The figure shows the evolution of some random initial configurations.*

automata a very interesting approach to model physical systems and in particular to simulate complex and nonequilibrium phenomena.

The studies undertaken by S. Wolfram in the 1980s [10,2] clearly estalishes that a CA (the famous Wolfram's rules) may exhibits many of the behaviors encountered in continuous systems, yet in a much simpler mathematical framework. A further step is to recognize that CAs are not only behaving similarly to some dynamical processes, they can also represent an actual model of a given physical system, leading to macroscopic predictions that could be checked experimentally. This fact follows from statistical mechanics which tells us that the macroscopic behavior of many systems is quite disconnected from its microscopic reality and that only symmetries and conservation laws survives to the change of observation level: it is well known that the flows of a fluid, a gas or even a granular media are very similar at a macroscopic scale, in spite of their different microscopic nature. Figure 2 show some typical behavior of the simplest Wolfram rules that have been classified in four group, accoding to their degree of complexity.

An interesting example is the FHP fluid model proposed by Frisch, Hasslacher and Pomeau in 1986[11] which can be viewed as a fully discrete molecular dynamics and yet behaves as predicted by the Navier-Stokes equation when the observation time and length scales are much larger than the lattice and automaton time step.

Cellular automata fluids like the FHP model (or lattice gas automata (LGA) as these models are often termed), cannot directly compete with standard computational fluid dynamics techniques for high Reynolds flows. However, they have been very successful to model complex situations for which traditional computing techniques are hardly applicable. Flows in porous media [12–14], immiscible flows and instabilities [15–18], spreading of a liquid droplet and wetting phe-

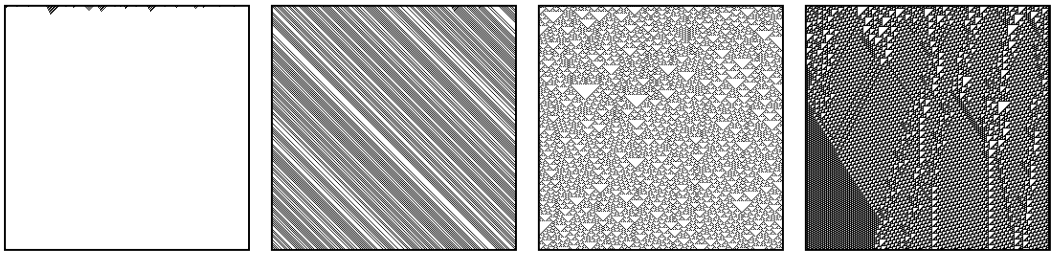

Figure 2: *Example of four Wolfram rules with a random initial configuration. Horizontal lines correspond to consecutive iterations. The initial state is the uppermost line. (a) Rule 40 belonging to class 1 reaches very quickly a fixed point (stable configuration). (b) Rule 56 of class 2 reaches a pattern composed of stripes which move from left to right. (c) Rule 18 is in class 3 and exhibits a self-similar pattern. (d) Rule 110 is an example of a class 4 cellular automaton. Its behavior is not predictable and as a consequence, we observe a rupture in the pattern, on the left part.*

nomena [3,19], granular flows[20,21] microemulsion [22] erosion and transport problems [3,23] are some examples pertaining to fluid dynamics.

Other physical situations, like pattern formation, reaction-diffusion processes [24–26], nucleation-aggregation growth phenomena, traffic process [27–29] are very well suited to the cellular automata approach.

The cellular automata paradigm presents some weaknesses inherent to its discrete nature. Lattice Boltzmann (LB) models have been proposed to remedy some of these problems, using real-valued states instead of Boolean variables. It turns out that LB models are indeed a very powerful approach which combines numerical efficiency with the advantage of having a model whose microscopic components are intuitive.

This paper is organized as follows. In the remaining of section 1 a precise definition of a cellular automata is given. We present some argument to justify the approach and, finally, the advantages and drawbacks of the method are outlined. In section 2, a sampler of CA rules are presented in order to illustrate the methodology and give an account of the large variety of possible applications. Section 3 shows, for the case of a fluid, how to derive rigorously the macroscopic behavior of a cellular automata model, starting from its Boolean dynamics. Section 4 discusses the lattice Boltzmann (LB) method and presents an application to compute deposition patterns in snow transport. Section 5 is devoted to reaction-diffusion systems and some examples of pattern formations. In section 6 we introduce multiparticles models that concile some of the advantages of the CA and LB approaches. Finally, section 7 proposes a LB model for wave propagation in heterogeneous media, as well as its application to model a

fracture process and wave localization.

1.3 Definition

In order to give a definition of a cellular automaton, we first present a simple example. Although it is very basic, the rule we discuss here exhibits a surprisingly rich behavior. It has been proposed initially by Edward Fredkin in the 1970s [30] and is defined on a two-dimensional square lattice.

Each site of the lattice is a cell which is labeled by its position $\vec{r} = (i, j)$ where i and j are the row and column indices. A function $\psi_t(\vec{r})$ is associated to the lattice to describe the state of each cell at iteration t. This quantity can be either 0 or 1.

The cellular automata rule specifies how the states ψ_{t+1} are to be computed from the states at iteration t. We start from an initial condition at time $t = 0$ with a given configuration of the values $\psi_0(\vec{r})$ on the lattice. The state at time $t = 1$ will be obtained as follows

(1) Each site $\vec{r}$ computes the sum of the values $\psi_0(\vec{r}')$ on the four nearest neighbor sites $\vec{r}'$ at north, west, south and east. The system is supposed to be periodic in both i and j directions (like on a torus) so that this calculation is well defined for all sites.

(2) If this sum is even, the new state $\psi_1(\vec{r})$ is 0 (white) and, else, it is 1 (black).

The same rule (steps 1 and 2) is repeated over to find the states at time $t = 2, 3, 4, ...$

From a mathematical point of view, this cellular automata parity rule can be expressed by the following relation

$$\psi_{t+1}(i,j) = \psi_t(i+1,j) \oplus \psi_t(i-1,j) \oplus \psi_t(i,j+1) \oplus \psi_t(i,j-1) \qquad (1)$$

where the symbol $\oplus$ stands for the exclusive OR logical operation. It is also the sum modulo 2: $1 \oplus 1 = 0 \oplus 0 = 0$ and $1 \oplus 0 = 0 \oplus 1 = 1$.

When this rule is iterated, very nice geometric patterns are observed, as shown in figure 3. This property of generating complex patterns starting from a simple rule is generic of many cellular automata rules. Here, complexity results from some spatial organization which builds up as the rule is iterated. The various contributions of successive iterations combine together in a specific way. The spatial patterns that are observed reflect how the terms are combined algebraically.

This example shows that despite the simplicity of the local rule, the global behavior of a CA model can be quite complex. In the present case, the mechanisme yielding these complex patterns can be unraveled by working out how successive iterations combine several copies of the initial configuration, all shifted by a different amount[3].

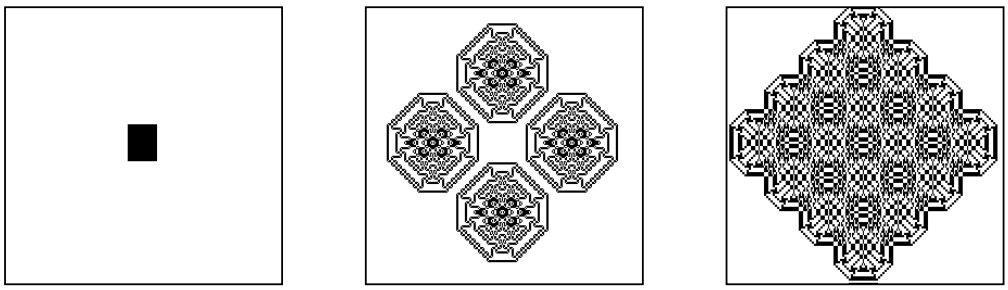

Figure 3: *The $\oplus$ rule on a 256×256 periodic lattice. (a) initial configuration. (b) and (c) configurations after $t_b = 93$ and $t_c = 110$ iterations, respectively.*

Based on this example we now give a definition of a cellular automata. Formally a cellular automata is made of

(i) A regular lattice of cells covering a portion of a d-dimensional space.

(ii) A set $\mathbf{\Phi}(\vec{r}, t) = \{\Phi_1(\vec{r}, t), \Phi_2(\vec{r}, t), ..., \Phi_m(\vec{r}, t)\}$ of boolean variables attached to each site $\vec{r}$ of the lattice and giving the local state of each cell at the time $t = 0, 1, 2, ...$

(iii) A rule $\mathbf{R} = \{R_1, R_2, ..., R_m\}$ which specifies the time evolution of the states $\mathbf{\Phi}(\vec{r}, t)$ in the following way

$$\Phi_j(\vec{r}, t + \tau) = R_j(\mathbf{\Phi}(\vec{r}, t), \mathbf{\Phi}(\vec{r} + \vec{\delta}_1, t), \mathbf{\Phi}(\vec{r} + \vec{\delta}_2, t), ..., \mathbf{\Phi}(\vec{r} + \vec{\delta}_q, t)) \quad (2)$$

where $\vec{r} + \vec{\delta}_k$ designate the cells belonging to a given neighborhood of cell $\vec{r}$.

The example discussed in the previous section is a particular case in which the state of each cell consists of a single bit $\Phi_1(r, t) = \psi_t(\vec{r})$ of information and the rule is the addition modulo 2.

In the above definition, the rule $\mathbf{R}$ is identical for all sites and is applied simultaneously to each of them, leading to a synchronous dynamics. It is important to notice that the rule is *homogeneous*, that is it cannot not depend explicitly on the cell position $\vec{r}$. However, spatial (or even temporal) inhomogeneities can be introduced anyway by having some $\Phi_j(\vec{r})$ systematically 1 in some given locations of the lattice to mark particular cells on which a different rule apply. Boundary cells are a typical example of spatial inhomogeneities. Similarly, it is easy to alternate between two rules by having a bit which is 1 at even time steps and 0 at odd time steps.

The neighborhood (i.e. the spatial region around each cell used to compute the next state) is usually made of the adjacent cells of the central cell. It is

often restricted to the nearest or next to nearest neighbors, otherwise the complexity of the rule is too large. For a two-dimensional cellular automaton, two neighborhoods are often considered: the von Neumann neighborhood which consists of a central cell (the one which is to be updated) and its four geographical neighbors North, West, South and East. The Moore neighborhood contains, in addition, the second nearest neighbor North-East, North-West, South-East and South-East, that is a total of nine cells.

According to the above definition, a cellular automaton is deterministic. The rule **R** is some well defined function and a given initial configuration will always evolve identically. However, as we shall see later, it may be very convenient for some applications to have a certain degree of randomness in the rule. For instance, it may be desirable that a rule selects one outcome among several possible states, with a probability p. Cellular automata whose updating rule is driven by some external probabilities are called *probabilistic* cellular automata. On the other hand, those which strictly comply with the definition given above, are referred to as *deterministic* cellular automata.

Probabilistic cellular automata are a very useful generalization because they offer a way to adjust the parameters of a rule in a continuous range of values, despite the discrete nature of the cellular automata world. This is very convenient when modeling physical systems in which, for instance, particles are annihilated or created at some given rate.

1.4 Limitations, advantage, drawbacks and Extension

Modeling a system at a microscopic level of description has significant advantages. The interpretation of the cellular automata dynamics in terms of simple microscopic rules offers a very intuitive and powerful approach to model phenomena that are very difficult to include in more traditional approaches (such as differential equations). For instance, boundary conditions are often naturally implemented in a cellular automata model because it has a natural interpretation at this level of description (e.g. particles bouncing back on an obstacle). For instance, the phenomena of wetting of a solid substrate by a spreading liquid illustrates the difficulty to define appropriate boundary conditions at the level of the Navier-Stokes equation. Yet, in the framework of a CA description, this can be achieved in a simple way [3].

Numerically, an advantage of the CA approach is its simplicity and its adequation to computer architectures and parallel machines. In addition, working with Boolean quantities prevent numerical instabilities since an exact computation is made. There is no truncation or approximation in the dynamics itself. Finally, a CA model is an implemetation of a N-body system where all correlations are taken into account, as well as spontaneous fluctuations arising in a system made up of many particles.

On the other hand, cellular automata models have several drawbacks related

to their fully discrete nature. An important one is the statistical noise requiring a systematic averaging processes. Another one is the little flexibility to adjust parameters of a rule in order to describe a wider range of physical situations.

At the end of the 1980s, McNamara and Zanetti [31] Higueras, Jimenez and Succi [32] have shown the advantage of extending the Boolean dynamics of the automaton to directly work on real numbers representing, somehow, the probability for a cell to have a given state. This approach, called the lattice Boltzmann (LB) method, is numerically much more efficient than the Boolean dynamics and provides an new computational model much more appropriate to simulate high Reynolds flows and many other relevant applications (for instance glacier flow[33] and fracture processes). On the other hand, the LB approach re-introduce the risk of numerical instabilities and, also, requires some hypotheses of factorization of the joint probability in order to write the interaction. See [3] for more detail.

Another generalization of the original definition of a CA is the multiparticle method in which the number of state of each cell is infinite so that an arbitrary number of particles can stay simultaneously at each site. This offers much more flexibility to tune the parameter of the rule and reduces considerably the statistical noise. A multiparticle model goes in the same direction as the LB models but it does not need a factorization assumption and is not sensitive to numerical instability. Unfortunately, it requires more implementation effort than the LB approach and is also numerically less efficient [3].

Finally, we should remark that the cellular automata approach is not a rigid framework but should allow for many extensions according to the problem at hand. The CA methodology is a philosophy of modeling where one seeks a description in terms of simple but essential mechanisms. Its richness and interest of comes from the microscopic contents of its rule for which there is, in general, a clear physical or intuitive interpretation of the dynamics directly at the level of the cell.

2 Examples of simple rules

In this section we consider several CA rules in order to illustates the ideas we have introduced in section 1. Although the rules we will present here have a clear physical contents, some of them should be considered as toy models because their ability to describe the macroscopic behavior of a real physical system does not resist to a detailled analysis. However, our goal is to present the flavor of the CA appraoch but not to give a proof that the rule we propose is rigorously related to a given process. More CA applications are discussed in [3]

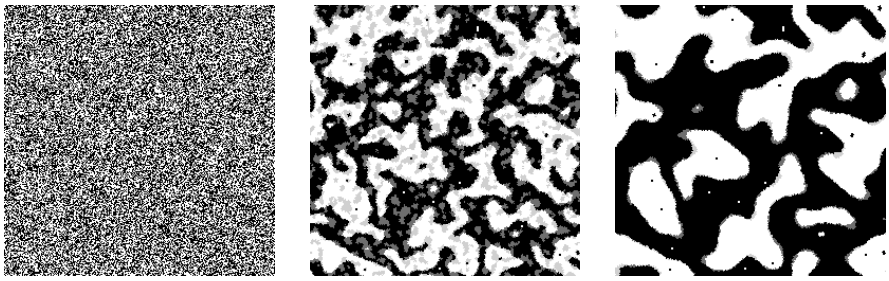

Figure 4: *Evolution of the annealing rule. The inherent "surface tension" present in the rule tends to separate the black phases $s = 1$ from the white phase $s = 0$. The snapshots (a), (b) and (c) correspond to $t = 0$, $t = 72$ and $t = 270$ iterations, respectively. The extra gray levels indicate how "capes" have been eroded and "bays" filled: dark gray shows the black regions that have been eroded during the last few iterations and light gray marks the white regions that have been filled.*

2.1 A growth model

A natural class of cellular automata rules consists of the so-called *majority rules*. The updating selects the new state of each cell so as to conform to the value currently hold by the majority of the neighbors. Typically, in these majority rules, the state is either 0 or 1.

A very interesting behavior is observed with the twisted majority rule proposed by G. Vichniac [34]: in two-dimensions, each cell considers its Moore neighborhood (i.e itself plus its eight nearest neighbors) and computes the sum of the cells having a value 1. This sum can be any value between 0 and 9. The new state $s_{ij}(t+1)$ of each cell is then determined from this local sum, according to the following table

$$\begin{array}{ll} \mathrm{sum}_{ij}(t) & 0\ 1\ 2\ 3\ 4\ 5\ 6\ 7\ 8\ 9 \\ s_{ij}(t+1) & 0\ 0\ 0\ 0\ 1\ 0\ 1\ 1\ 1\ 1 \end{array} \qquad (3)$$

As opposed to the plain majority rule, here, the two middle entries of the table have been swapped. Therefore, when there is a slight majority of 1 around a cell, it turns to 0. Conversely, if there is a slight majority of 0, the cell becomes 1.

Surprisingly enough this rule describes the interface motion between two phases, as illustrated in Figure 4. Vichniac has observed that the normal velocity of the interface is proportional to its local curvature, as required by the Allen-Cahn [35] equation. Of course, due to its local nature, the rule cannot detect the curvature of the interface directly. However, as the the rule is iterated, local information is propagated to the nearest neighbors and the radius of curvature emerges as a collective effect.

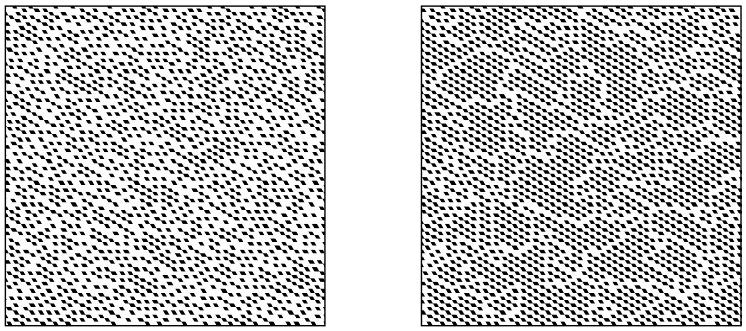

Figure 5: *Final (stationary) configuration of the competition CA model. (a) A typical situation with about 23% of active cells, obtained with almost any value of p_{anihil} and p_{growth}. (b) Configuration obtained with $p_{anihil} = 1$ and $p_{growth} = .8$ and yielding a fraction of 28% of active cells; one clearly sees the close-packed regions and the defects.*

This rule is particularly interesting when the initial configuration is a random mixture of the two phases, with equal concentration. Otherwise, some pathological behaviors may occur. For instance, an initial square of 1's surrounded by zero's will not evolve: right angles are not eroded but stable structures.

2.2 Competition models and cell differentiation

In section 2.1 we have discussed a majority rule in which the cells imitate their neighbors. In some sense, this corresponds to a cooperative behavior between the cells. A quite different situation can be obtained if the cells obey a competitive dynamics. For instance we may imagine that the cells compete for some resources at the expense of their nearest neighbors. A winner is a cell of state 1 and a looser a cell of state 0. No two winner cells can be neighbor and any looser cell must have at least one winner neighbor (otherwise nothing would have prevented it to also win).

It is interesting to note that this problem has a direct application in biology, to study cells differentiation. It has been observed in the development of the drosophila that about 25% of the cells forming the embryo are evolving to the state of neuroblast, while the remaining 75% does not. How can we explain this differentiation and the observed fraction since, at the beginning of the process all cells can be assumed equivalent? A possible mechanism [36] is that some competition takes place between the ajacent biological cells. In other word, each cell produces some substance S but the production rate is inhibited by the amount of S already present in the neighboring cells. Differentiation occurs when a cell reaches a level of S above a given threshold.

The competition CA model we propose to describe this situation is the follow-

ing. Due to the analogy with the biological system, we shall consider a hexagonal lattice which is a reasonable approximation of the cell arrangement observed in the drosophila'embryo. We assume that the values of S can be 0 (inhibited) or 1 (active) in each lattice cell.

- A $S = 0$ cell will grow (i.e. turn to $S = 1$) with probability p_{grow} provided that all its neighbors are 0. Otherwise, it stays inhibited.
- A cell in state $S = 1$ will decay (i.e. turn to $S = 0$) with probability p_{decay} if it is surrounded by at least one active cell. If the active cell is isolated (all the neighbors are in state 0) it remains in state 1.

The evolution stops (stationary process) when no $S = 1$ cell feels any more inhibition from its neighbor and when all $S = 0$ cell are inhibited by their neighborhood. Then, cells with $S = 1$ are those which will differentiate.

What is the expected fraction of these $S = 1$ cells in the final configuration? Clearly, the maximum value is 1/3 which, according to the inhibition condition we imposed, is the close-packed situation on the hexagonal lattice. On the other hand, the minimal value is 1/6, corresponding to a situation where the lattice is partitioned in blocks with one active cell surrounded by 5 inhibited cells. In practice we do not expect any of these two limits to occur spontanously after the automaton evolution. On the contrary, we should observe clusters of close-packed active cells surrounded by defects, i.e. regions of low density of active cells (see figure 5).

CA simulations give a very interesting results, namely that the fraction s of active cells when the stationary state is reached is

$$.23 \leq s \leq .24$$

almost irrespectively of the values chosen for p_{anihil} and p_{growth}. This is exactly what we expect from the biological observations made on the drosophila's embryo. Thus, cell differentiation can be explained by a geometrical competition without having to specify the inhibitory couplings between adjacent cell and the production rate (i.e. the values of p_{anihil} and p_{growth}): the result is quite robust against any possible choices.

In our CA model, there are, however, some pathological results when either p_{anihil} or p_{growth} equals to one. For instance, $p_{anihil} = 1$ and $p_{growth} = .8$, we obtain $s \approx .28$. This situation is illustrated in figure 5 (b).

2.3 Traffic models

Cellular automata models for road traffic have received a great deal of interest during the past few years (see [37,27–29,38–41] for instance).

2.3.1 One-dimensional models

One-dimensional models for single lane car motions are quite simple and elegant. The road is represented as a line of cells, each of them being occupied or not by a vehicle. All cars travel in the same direction (say to the right). Their positions are updated synchronously. During the motion, each car can be at rest or jump to the nearest neighbor site, along the direction of motion. The rule is simply that a car moves only if its destination cell is empty. This means that the drivers are short-sighted and do not know whether the car in front will move or is also stuck by another car. Therefore, the state of each cell s_i is entirely determined by the occupancy of the cell itself and its two nearest neighbors s_{i-1} and s_{i+1}. The motion rule can be summarized by the following table, where all eight possible configurations $(s_{i-1}s_is_{i+1})_t \to (s_i)_{t+1}$ are given

$$\underbrace{(111)}_{1}\ \underbrace{(110)}_{0}\ \underbrace{(101)}_{1}\ \underbrace{(100)}_{1}\ \underbrace{(011)}_{1}\ \underbrace{(010)}_{0}\ \underbrace{(001)}_{0}\ \underbrace{(000)}_{0} \tag{4}$$

This cellular automaton rule turns out to be Wolfram's rule 184 [10,37].

This simple dynamics captures an interesting feature of real car motion: traffic congestion. Suppose we have a low car density ρ in the system, for instance something like

$$\ldots 0010000010010000010\ldots \tag{5}$$

This is a *free* traffic regime in which all the cars are able to move. The average velocity $< v >$ defined as the number of motions divided by the number of cars is then

$$< v_f >= 1 \tag{6}$$

where the subscript f indicates a free state. On the other hand, in a high density configuration such as

$$\ldots 110101110101101110\ldots \tag{7}$$

only 6 cars over 12 will move and $< v >= 1/2$. This is a partially jammed regime.

If the car positions were uncorrelated, the number of moving cars (i.e the number of particle-hole pairs) would be given by $L\rho(1-\rho)$, where L is the system size. Since the number of cars is ρL, the average velocity would be

$$< v_{\text{uncorrel}} >= 1 - \rho \tag{8}$$

However, in this model, the car occupancy of adjacent sites is highly correlated and the vehicles cannot move until a hole has appeared in front of them. The car distribution tries to self-adjust to a situation where there is one spacing between consecutive cars. For densities less than one-half, this is easily realized and the system can organize to have one car every other site.

Therefore, due to these correlations, equation 8 is wrong in the high density regime. In this case, since a car needs a hole to move to, we expect that the

number of moving cars simply equals the number of empty cells [37]. Thus, the number of motions is $L(1-\rho)$ and the average velocity in the jammed phase is

$$< v_j >= \frac{1-\rho}{\rho} \tag{9}$$

A richer version of the above CA traffic model is due to Nagel and Schreckenberg [40,27,28]. The cars may have several possible velocities $u = 0, 1, 2, ..., u_{max}$. Let u_i be the velocity of car i and d_i the distance, along the road, separating cars i and $i+1$. The updating rule is:

- The cars accelerate when possible: $u_i \rightarrow u_i' = u_i + 1$, if $u_i < u_{max}$.
- The cars slow down when required: $u_i' \rightarrow u_i'' = d_i - 1$, if $u_i' \geq d_i$.
- The cars have a random behavior: $u_i'' \rightarrow u_i''' = u_i'' - 1$, with probability p_i if $u_i'' > 0$.
- Finally the cars move u_i''' sites ahead.

This rule caputres some important behaviors of real traffic on a highway: velocity fluctuations due to a non-deterministic behavior of the drivers, and "stop-and-go" waves observed in high density traffic regime (i.e. some cars get stop for no specific reasons.

2.3.2 A 2D traffic model

A CA traffic model can also be defined for the situation of a street network, where several lane may cross provided that the rule is extended to deal with cars entering the same road junction. In the case of an urban traffic, we may restrict ourselves to a one speed CA.

Our approach is to model a road intersection as a rotary. Cars in the rotary have priority over those willing to enter. It is easy to add traffic lights in such a model by blocking the entry to the rotary to to car coming from a given road. Note that road crossings may be a bottleneck limiting the traffic flow and, thus, causing congestion.

Let us consider the case of a Manhattan-like city. We assume that horizontal roads consist of two lanes, one for eastward motion and the other for westward motion. Similarly, vertical streets are composed of northbound and southbound lanes. Road junctions are formed by central points around which the traffic moves always in the same direction.

A four-corner junction is shown in figure 6. The four middle cells constitute the rotary. A vehicle on the rotary (like b or d) can either rotate counterclockwise or exit. A local flag t_f is used to decide of the motion of a car in a rotary. If $t_f = 0$, the vehicle (like d) exits in the direction allowed by the color of its lane

(see figure caption). If $t_f = 1$, the vehicle moves counterclockwise, like b. The value of the local turn flag t_f can be updated according to the modeling needs: it can be constant for some amount of time to impose a particular motion at a given junction, completely random, random with some bias to favor a direction of motion, or may change deterministically according to any user specified rule.

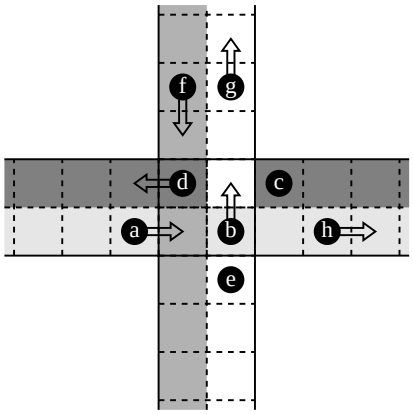

Figure 6: *Example of a traffic configuration near a junction. The four central cells represent a rotary which is traveled counterclockwise. The grey levels indicate the different traffic lanes: white is a northbound lane, light grey an eastbound lane, grey a southbound lane and, finally, dark grey is a westbound lane. The dots labeled a, b, c, d, e, f, g and h are cars which will move to the destination cell indicated by the arrows, as determined by the cell turn flag t_f. Cars without an arrow are forbidden to move.*

Figure 7 shows a typical traffic configurations. In figure (a), a vehicle has a probability 1/2 to exit at each rotary cell. In figure (b), the turn flag t_f has an initial random distribution on the rotary. This distribution is fixed for the first 20 iterations and then flips to $t_f = 1 - t_f$ for the next 20 steps an so on. In this way, a junction acts as a kind of traffic light, which for some amount of time, allows only a given flow pattern. We observed that the global traffic pattern is different in the two cases: in case (a), the car distribution is quite homogeneous along the streets. On the other hand, in case (b), cars get queued at some junctions while some other streets remain empty.

The behavior of the above traffic model can be described analytically [29]. The first important fact is that a rotary junction has a maximum possible flow of cars. Thus, the number of vehicles able to enter a rotary per unit time cannot be larger than a given value determined by the rule of motion. Therefore, there is a critical average density ρ_1^{crit} above which the traffic is not free but constrained by this maximum rotary flow. As a result, car queues are formed at road junctions.

The second key observation is that, in the regime above ρ_1^{crit}, the system self-organizes in three different regions of fixed car densities: the queues that form

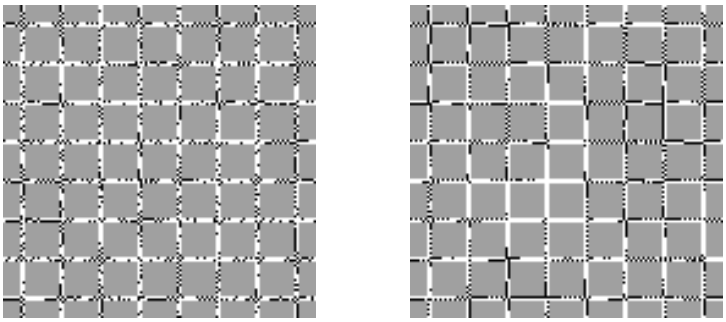

Figure 7: *Traffic configuration after 600 iterations, for a car density of 30%. Streets are white, buildings grey and the black pixels represent the cars. The Situation (a) corresponds to an equally likely behavior at each rotary junction, whereas image (b) mimics the presence of traffic lights. In the second case, queues are more likely to form and the global mobility is less than in the first case.*

before a junction, the road segments after a junction, characterized by a low traffic density and the region inside a rotary. The three densities associated to these different regions correspond to a jammed density ρ_j, a free traffic density ρ_f and a rotary density ρ_r, respectively.

As the overall car number is increased, ρ_j, ρ_f and ρ_r remain constant: the result of increasing the number of cars is to extend the length ℓ of the car queues, without changing the density in the three regions. The reason for fixed densities is that, due to the flow diagram of rule 184 [37], there are only two possible densities ρ_f and ρ_j compatible with a given traffic flow $\rho < v >$, along a road segment. Thus, the only way to absorb an excess of car is to increase the size of the queue.

When one keeps adding cars in the system, there is a second critical average density ρ_2^{crit} for which the length of some queues becomes larger than the distance separating two consecutive street intersections. The up-traffic rotary output gets disturbed and, from a maximum-flow traffic regime, one gets into a strongly jammed phase.

Provided that the turning decision at rotaries is random and not time correlated, one typically obtains [29]

$$\rho_f = \frac{1}{4} \qquad \rho_j = \frac{3}{4} \qquad \rho_r = \frac{1}{2} \tag{10}$$

Assuming that the queues length is ℓ along all road segments and that the separation between two consecutive junctions is L (the network period), we can relate the average car density ρ to ℓ by the relation[37]

$$4(L-2-\ell)\rho_f + 4\ell\rho_j + 4\rho_r = 4L\rho \tag{11}$$

Equation 11 simply reflects that the total number of cars is distributed in three regions: queues of length ℓ and density ρ_j, free traffic segments of length $L-\ell-2$ and density ρ_f and rotaries of size four and density ρ_r.

In the case of large L, the queue length can be approximated by

$$\frac{\ell}{L} = \frac{\rho - \rho_f}{\rho_j - \rho_f} \tag{12}$$

Equation 12 provides a way to determine the critical densities ρ_1^{crit} and ρ_2^{crit}. For $\rho < \rho_f$, ℓ is negative, which should be interpreted in the sense that no queue is formed. This is the free traffic regime. Thus, $\rho_1^{crit} = \rho_f = 1/4$ and the average velocity is $< v >= 1$, independent of ρ.

On the other hand, for $\rho_f < \rho < \rho_j$, car queues form but their lengths are smaller than the distance between successive intersections. This is the maximum flow regime. In this case, we have $\rho < v >= J = \text{const} = 1/4$, that is $< v >= 1/(4\rho)$.

Finally, for $\rho > \rho_j = \rho_2^{crit}$, the queues reach their maximum length L and the rotary exits are hindered. This is the strongly jammed traffic regime. The traffic velocity is governed by the motion of holes and obeys 9, namely $< v >= (1-\rho)/\rho$. If $< v >$ is taken as the order parameter, both of these transitions are second order.

Figure 8 (a) shows the velocity-density diagram obtained from CA simulations, for the situation we just described. We have considered various road spacings for our measurements (i.e the distance L separating consecutive intersections). The larger the spacing the better the agreement with the analytical description. Note that for small L, the correlation along the lane cannot build up and $< v >$ obeys 8.

In figure 8 (b), we also show the velocity-density diagram in the case the drivers choose the rotary exit at random but stick to this decision even if the exit they have chosen is not free.

The present CA model can be adapted to simulate traffic in more realistic situations. We have considered the case of the city of Geneva and its suburbs[42,43]. The simulations uses the full road network (4000 km, 3145 road segments and 1066 junctions with a number of 800765 cells) and a large set of origin and destination pairs (about 50'000) for the cars traveling during the rush hour.

The precise departure time of each vehicle is not known from observations. It is natural to assume that the distribution of these departure times is not uniform. Here we assume that this distribution has the form shown in figure 9 and is characterized by two parameters: (i) the duration I of the departure period and (ii) the ratio p_2/p_1 specifying the degree of non-uniformity. Empirically we choose $p_2/p_1 = 6$ and $I = 45$ minutes (so that almost all cars have arrived after 90 minutes).

Due to the lack of data concerning the real evolution of the traffic state in the city of Geneva, we did not investigate systematically the effect of varying p_2/p_1

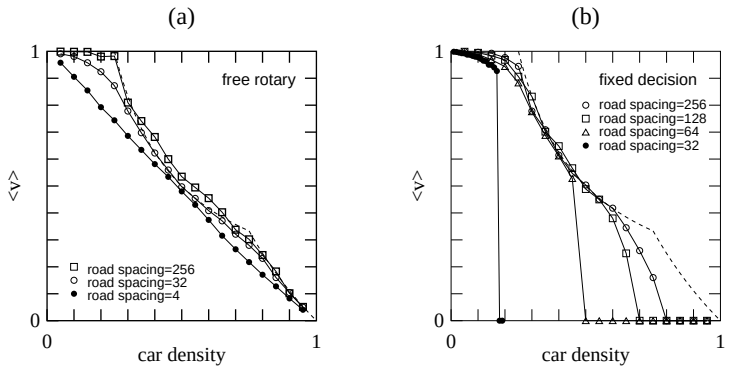

Figure 8: *Average velocity versus average density for the cellular automata street network, for (a) time-uncorrelated turning strategies and (b) a fixed driver's decision. The different curves correspond to different distances L between successive road junctions. The dashed line is the analytical prediction. Junction deadlock is likely to occur in (b), resulting in a completely jammed state.*

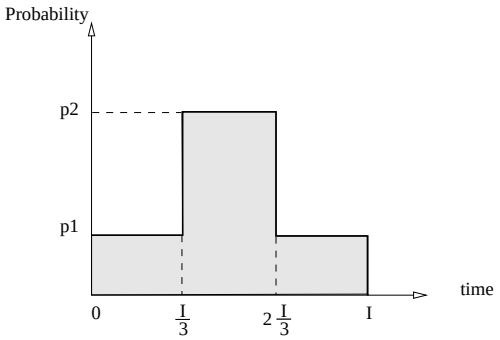

Figure 9: *Distribution of departure times used in the simulation of the city of Geneva traffic.*

and I. Rather, we focused on the problem of measuring the time necessary for a test car to travel from a given origin A to a given destination B. This time is of direct interest to the drivers because it determines, for instance, when they must leave their house in order to be on time at their work. This is also a quantity which is easily comparable with the reality by actually driving from A to B.

The interesting fact is that the travel time is a fluctuating quantity. If one repeats the same trip under the same condition (for instance the next day, at the same time), the drive is likely to be longer or shorter. This fact is well known from everyday experience and is also well reproduced in the CA model because the probability distribution of the departure times gives the necessary randomness to produce fluctuations when the simulation is repeated.

Our main result is that the amplitude of the variations of the travel times depends very much on the departure time of the test car and on its trip. In the

simulations, we studied the four trips shown in figure 10.

The measured times obtained from the simulation for trips 2 and 3 are shown in figure 11. The results for trip 1 and 4 are similar.

For trip 3, the average time needed to reach the desired destination is not constant: it is maximal if the driver leaves 15 to 20 minutes after the start of the rush hour. It is minimal if the diver leaves at the very beginning or the very end of interval I. On the other hand, the average time for trip 2 is quite stable. These two situations differ by the fact that trip 3 uses heavily loaded sections with many crossings while trip 2 uses higher capacity sections.

We also observe that, for trip 3, it is impossible to make accurate predictions on the time needed to reach the destination point. Variations up to 30% show up. We call this variation the *risk*[1] associated to the trip (for a given departure time) to describe the fact that an expected outcome is likely not to occur. In practice, for trip 3, in which the variation is high, there is a large risk to arrive late at destination, or to be too early, which may not be acceptable either. This also means that it is not possible to establish an accurate schedule for taxis or public transportation, unless dedicated lanes are available.

Finally, figure 12 shows the dependence of $< v >$, the average car velocity in the network, as a function of the average car density ρ. Since the traffic load is not stationary but concentrated within about one and a half hour, the steady-state density-velocity diagram (as shown for instance in fig. 8) is no longer valid and must be replaced by a "dynamic" diagram which shows a significant hysteresis.

2.4 A simple gas: the HPP model

The HPP rule is a simple example of an important class of cellular automata models: lattice gas automata (LGA). The basic ingredient of such models are point particles that move on a lattice, according to appropriate rules so as to mimic a fully discrete "molecular dynamics."

The HPP lattice gas automata is traditionally defined on a two-dimensional square lattice. Particles can move along the main directions of the lattice, as shown in figure 13. The model limits to 1 the number of particles entering a given site with a given direction of motion. This is the exclusion principle which is common in most LGA. Consequently, four bits of information in each site are enough to describe the system during its evolution. For instance, if at iteration t site $\vec{r}$ has the following state $s(\vec{r}, t) = (1011)$, it means that three particles are entering the site along direction 1,3 and 4, respectively.

The cellular automata rule describing the evolution of $s(\vec{r}, t)$ is often split in two steps: collision and motion (or propagation). The collision phase specifies how the particles entering the same site will interact and change their trajectories. The purpose of the HPP rule is to model a gas of colliding particles and, thus,

[1] In finance, the term risk is also used to describe the standard deviation of a random quantity.

Figure 10: *The road network of Geneva used in our simulation and the four selected trips considered to measure the travel time of a test car.*

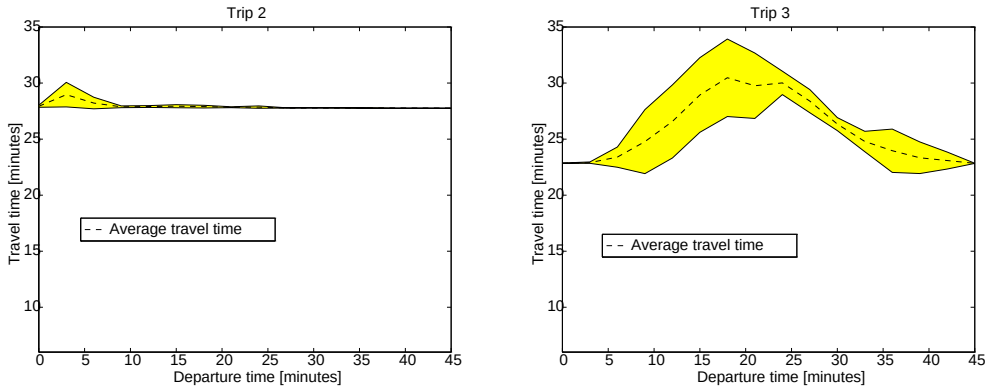

Figure 11: *Expectation time and "risk" of trips 2 and 3 of figure 10. The horizontal axis corresponds to the departure time of a test vehicle within interval I. The dashed line shows the average driving time and the shaded region indicates the amplitude of the variation of this time (computed as the standard deviation). Note that the times shown here are pretty realistic, thus giving an indirect validation of our simulations for the case of Geneva.*

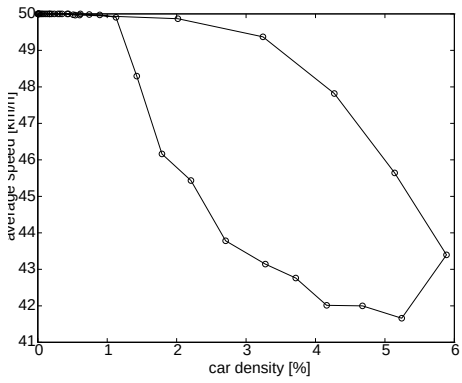

Figure 12: *Dynamical flow diagram for $p_2/p_1 = 6$. As time goes on ($t \in [0, I]$), the car density first increases and the upper branch of the diagram is formed; then, when the density decreases, the lower branch is measured.*

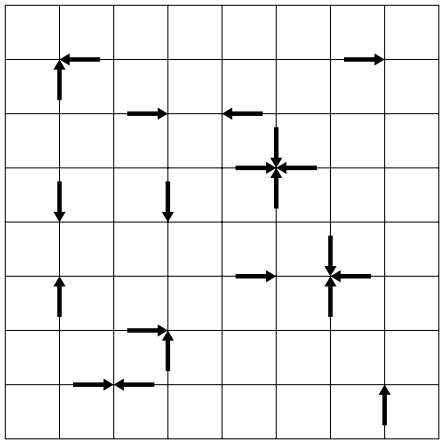

Figure 13: *Example of a configuration of HPP particles*

essential features of this step are borrowed from the real microscopic interactions, namely local conservation of momentum and particle number. Since the collision phase amounts to rearranging the particles in different direction, it ensures that the exclusion principle will be satisfied, provided that it was at time $t = 0$.

During the propagation phase, the particles actually move to the nearest neighbor site they are traveling to. Figure 14 illustrates the HPP rules. This decomposition into two phases is a quite convenient way to partition the space so that the collision rule is purely local.

According to our Boolean representation of the particles at each site, the collision part for the two head on collisions are expressed as

$$(1010) \rightarrow (0101) \qquad (0101) \rightarrow (1010) \tag{13}$$

all the other configurations being unchanged. During the propagation phase, the first bit of the state variable is shifted to the east neighbor cell, the second bit to the north and so on.

The aim of this rule is to reproduce some aspect of the real interactions between particles, namely that momentum and particle number are conserved during a collision. From figure 14, it is easy checked that these properties are obeyed: a pair of zero momentum particles along a given direction is transformed into another pair of zero momentum along the perpendicular axis.

The HPP rule captures another important ingredient of the microscopic nature of a real interaction: invariance under time reversal. Figures 14 (b) and (c) show that, if at some given time, the directions of motion of all particles are reversed, the system will just trace back its own history. Since the dynamics of a deterministic cellular automaton is exact, this fact allows us to demonstrate the properties of physical systems to return to their original situation when all the particles reverse their velocity.

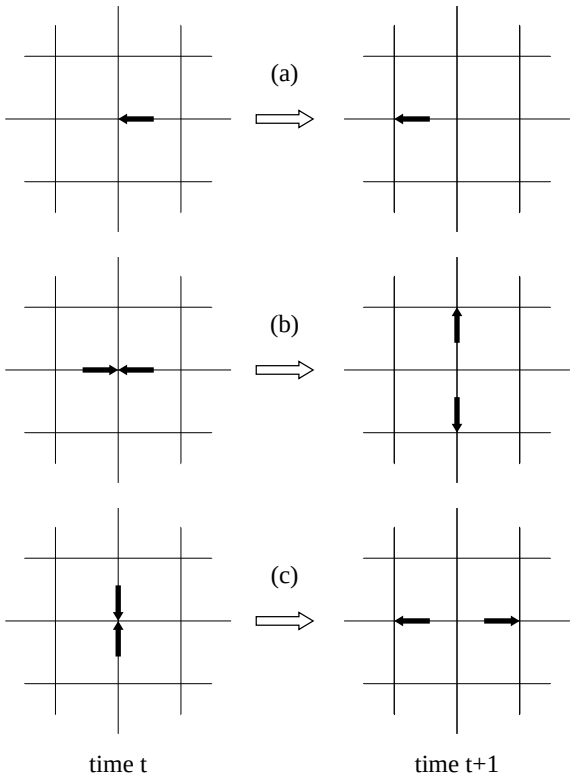

Figure 14: *The HPP rule: (a) a single particle has a ballistic motion until it experiences a collision; (b) and (c) the two non-trivial collisions of the HPP model: two particles experiencing a head on collision are deflected in the perpendicular direction. In the other situations, the motion is ballistic, that is the particles are transparent to each other when they cross the same site.*

Figure 15 illustrate the time evolution of a HPP gas initially confined in the left compartment of a container. There is an aperture on the wall of the compartment and the gas particles will flow so as to fill the entire space available to them. In order to include a solid boundary in the system, the HPP rule is modified as follows: when a site is a wall (indicated by an extra bit), the particles no longer experience the HPP collision but bounce back from where they came. Therefore, particles cannot escape a region delimited by such a reflecting boundary.

If the system of figure 15 is evolved, it reaches an equilibrium after a long enough time and no macroscopic trace of its initial state is any longer visible. However, no information has been lost during the process (no numerical dissipation) and the system has the memory of where it comes from. Reversing all the velocities and iterating the HPP rule makes all particle go back to the compartment in which they were initially located.

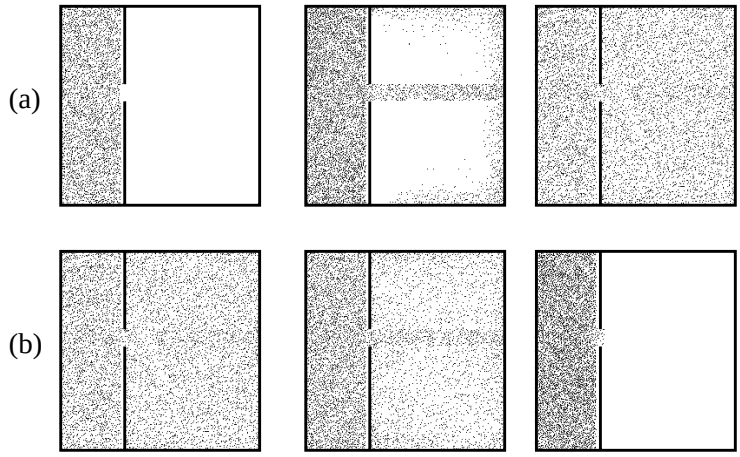

Figure 15: *Time evolution of a HPP gas. (a) From the initial state to equilibrium. (b) Illustration of time reversal invariance: in the rightmost image of (a), the velocity of each particle is reversed and the particles naturally return to their initial position.*

This behavior is only possible because the dynamics is perfectly exact and that no numerical errors are present in the numerical scheme. If one introduces externally some errors (for instance, one can add an extra particle in the system) before the direction of motion of each particle is reversed, then reversibility is lost.

The HPP rule is important because it contains the basic ingredients of many models we are going to discuss below. However, the capability of this rule to model a real gas of particle is poor, due to a lack of isotropy and spurious invariants. A remedy to this problem is to use a different lattice [3].

2.5 Random walk

The HPP rule we discussed in the previous section can be easily modified to produce many synchronous random walks. Instead of experiencing a mass and momentum conserving collision, each particle now selects, at random, a new direction of motion among the possible values permitted by the lattice. Since several particles may enter the same site (up to four, on a two-dimensional square lattice), the random change of directions should be such that there are never two or more particle exiting a site in the same direction. This would otherwise violate again the exclusion principle.

The solution is to shuffle the directions of motion or, more precisely, to perform a random permutation of the velocity vectors, independently at each lattice site and each time step. Figure 16 illustrate this probabilistic evolution rule. Note that at a macroscopic level of description, the random walk rule corresponds to a diffusion process.

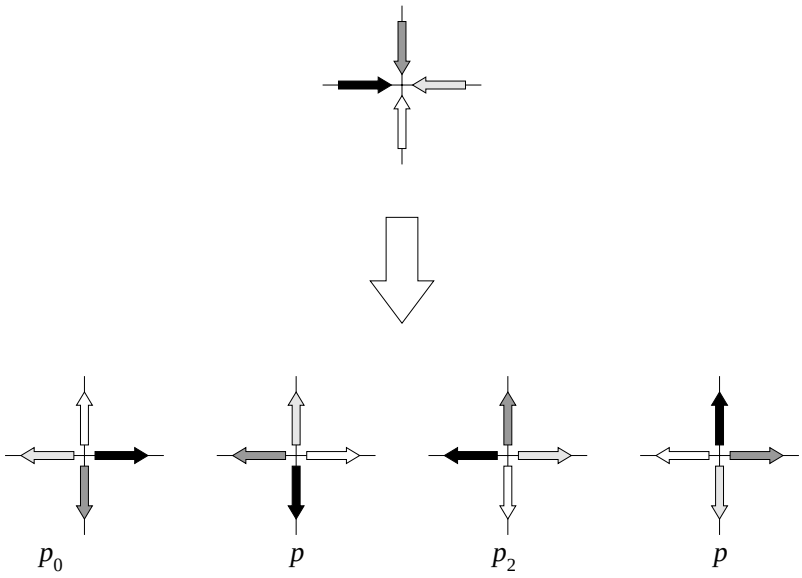

Figure 16: *How the entering particles are deflected at a typical site, as a result of the diffusion rule. The four possible outcomes occur with respective probabilities* p_0, p_1, p_2 *and* p_3. *The figure shows four particles, but the mechanism is data-blind and any one of the arrows can be removed when fewer entering particles are present.*

As an example of the use of the present random walk cellular automata rule, we discuss an application to growth processes. In many cases, growth is governed by a spatial quantity such as an electric field, a local temperature, or a particle density field [44]. Aggregation constitutes an important mechanism: like particles stick to each other as they meet and, as a result, form a complicated pattern with a branching structure.

A prototype model of aggregation is the so-called DLA model (diffusion-limited aggregation), introduced by Witten and Sander[45] in the early 1980s. Since its introduction, the DLA model has been investigated in great detail. However, diffusion-limited aggregation is a far from equilibrium process which is not described theoretically by first principle only. Spatial fluctuations that are typical of the DLA growth are difficult to take into account and a numerical approach is necessary to complete the analysis.

DLA-like processes can be readily modeled by our diffusion cellular automata, provided that an appropriate rule is added to take into account the particle-particle aggregation. The first step is to introduce rest particle to represent the particles of the aggregate. Therefore, in a two-dimensional system, a lattice site can be occupied by up to four diffusing particles, or by one "solid" particle. Our approach has some differences compared with the original Witten and Sanders model. All particles reside on a lattice and move simultaneously. They can stick

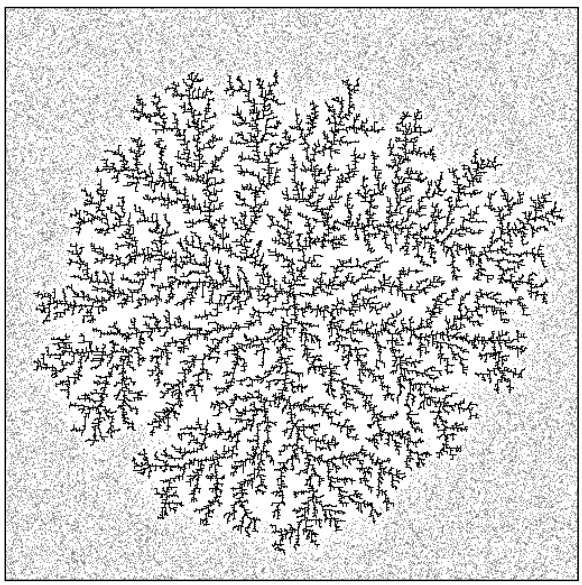

Figure 17: *Two-dimensional cellular automata DLA-like cluster (black), obtained with $p_s = 1$, an aggregation threshold of 1 particle and a density of diffusing particle of 0.06 per lattice direction. The gray dots represent the diffusing particles not yet aggregated.*

to different part of the cluster and we do not launch them, one after the other, from a region far away from the cluster. For this reason, we may expect some quantitative variation from the original DLA properties.

Figure 17 shows a two-dimensional DLA-like cluster grown by the cellular automata dynamics. At the beginning of the simulation, one or more rest particles are introduced in the system to act as aggregation seeds. The rest of the system is filled with particle with average concentration ρ. When a diffusing particle gets nearest neighbor to a rest particle, it stops and sticks to it by transforming into a rest particle. Since several particle can enter the same site, we may choose to aggregate all of them at once (i.e. a rest particle is actually composed of several moving particles), or to accept the aggregation only when a single particle is present.

In addition to this question, the sticking condition is important. If any diffusing particle always sticks to the DLA cluster, the growth is very fast and can be influenced by the underlying lattice anisotropy. It is therefore more appropriate to stick with some probability p_s. Since up to four particles may be simultaneously candidate for the aggregation, we can also use this fact to modify the sticking condition. A simple way is to require that the local density of particle be larger than some threshold (say 3 particles) to yield aggregation. The cluster shown in figure 17 has fractal dimension $d_f = 1.78$ which is not very different from the genuine, off-lattice DLA fractal dimension[46,44] $d_f = 1.70$.

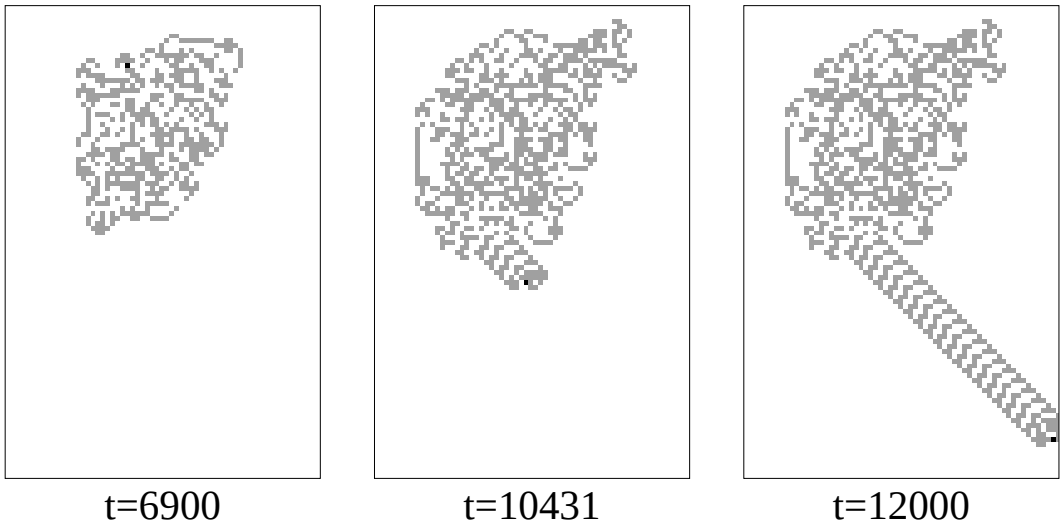

Figure 18: *The Langton's ant rule. The motion of a single ant starts with a chaotic phase of about 10000 time steps, followed by the formation of a highway. The figure shows the state of each lattice cell (gray or white) and the ant position (marked by the black dot). In the initial condition all cells are white and the ant is located in the middle of the image.*

2.6 The traveling ant

The ant rule is a cellular automata invented by Chris Langton[47] and Greg Turk which models the behavior of a hypothetical animal (ant) having a very simple algorithm of motion. The ant moves on a square lattice whose sites are either white or grey. When the ant enters a white cell, it turns 90 degrees to the left and paints the cell in gray. Similarly, if it enters a gray cell, it paints it in white and turn 90 degree to the right.

It turns out that the motion of this ant exhibits a very complex behavior. Suppose the ant starts in a completely white space. After a series of about 500 steps where it essentially keeps returning to its initial position, it enters a chaotic phase during which its motion is unpredictable. Then, after about 10000 steps of this very irregular motion, the ant suddenly performs a very regular motion which brings it far away from where it started.

Figure 18 illustrates the ant motion. The path the ant creates to escape the chaotic initial region has been called a highway[48]. Although this highway is oriented at 45 degrees with respect to the lattice direction, it is traveled by the ant in a way which makes very much think of a sewing machine: the pattern is a sequence of 104 steps which are repeated indefinitely.

The Langton ant is a good example of a cellular automata whose rule is very simple and yet generates a complex behavior which seems beyond our understand-

ing. Somehow, this fact is typical of the cellular automata approach: although we do know everything about the fundamental laws governing a system (because we set up the rules ourselves!), we are often unable to explain its macroscopic behavior.

There is anyway a global property of the ant motion: the ant visits an unbounded region of space, *whatever* the initial space texture is (configuration of gray and white cells).

The proof (due to Bunimovitch and Troubetzkoy) goes as follows: supposed the region the ant visits is bounded. Then, it contains a finite number of cells. Since the number of iteration is infinite, there is a domain of cells that are visited infinitely often. Moreover, due to the rule of motion, a cell is either entered horizontally (we call it a H cell) or vertically (we call it a V cell). Since the ant turns by 90 degrees after each step, a H cell is surrounded by four V cells and conversely. As a consequence, the H and V cells tile the lattice in a fixed checkerboard pattern. Now, we consider the upper rightmost cell of the domain, that is a cell whose right and upper neighbor is not visited. This cell exists if the trajectory is bounded. If this cell is an H cell (and be so for ever), it has to be entered horizontally from left and exited vertically downward and, consequently be gray. However, after the ant has left, the cell is white and there is a contradiction. The same contradiction appears if the cell is a V cell. Therefore, the ant trajectory is not bounded.

As it has been described, the above rule is defined only when a single ant moves on the lattice. We can easily generalize it when many ants are simultaneously present so that up to four of them may enter the same site at the same time, from different sides

Following the same idea as in the HPP rule, we will introduce $n_i(\vec{r},t)$ as a boolean variable representing the presence ($n_i = 1$) or the absence ($n_i = 0$) of an ant entering site $\vec{r}$ at time t along lattice direction $\vec{c}_i$, where $\vec{c}_1$, $\vec{c}_2$, $\vec{c}_3$ and $\vec{c}_4$ stand for direction right, up, left and down, respectively. If the color $\mu(\vec{r},t)$ of the site is gray ($\mu = 0$), *all* entering ants turn 90 degrees to the right. On the other hand, if the site is white($\mu = 1$), they all turn 90 degrees to the left. The color of each cell is modified after one or more ants have gone through. Here, we chose to switch $\mu \to 1 - \mu$ only when an odd number of ant are present.

When several ant travel simultaneously on the lattice, cooperative and destructive behaviors are observed. First, the erratic motion of several ants favors the formation of a local arrangement of colors allowing the creation of a highway. One has to wait much less time before the first highway appears. Second, once a highway is being created, other ants may use it to travel very fast (they do not have to follow the complicated pattern of the highway builder. In this way, the term "highway" is very appropriate. Third, a destructive effect occurs as the second ant gets to the highway builder. It breaks the pattern and several situations may be observed. For instance, both ants may enter a new chaotic motion; or the highway is traveled in the other direction (note that the rule is time reversal

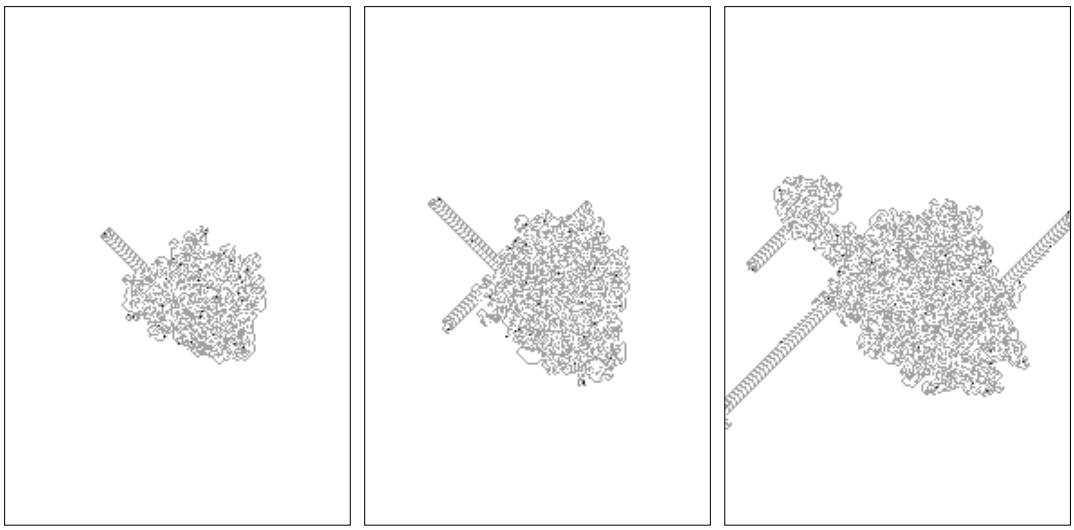

Figure 19: *Motion of several Langton's ants. Gray and white indicate the colors of the cells at the current time. Ant locations are marked by the black dots. At the initial time, all cells are white and a few ants are randomly distributed in the central region, with random directions of motion. The first highway appears much earlier than when the ant is alone. In addition the highway can be used by other ants to travel much faster. However, the "highway builder" is usually prevented from continuing its construction as soon as it is reached by the following ants. For instance, the highway heading north-west after 4900 steps get destroyed. A new highway emerges later on from the rest, as we see from the snapshot at time* $t = 8564$.

invariant) and destroyed. Figure 19 illustrates the multi-ant behavior.

The problem of an unbounded trajectory pauses again with this generalized motion. The assumption of Bunimovitch-Troubetzkoy's proof no longer holds in this case because a cell may be both an H or a V cell. Indeed, two different ants may enter a same cell one vertically and the other horizontally. Actually, the theorem of an unbounded motion is wrong in several cases where two ants are present. Periodic motions may occur when the initial positions are well chosen.

For instance, when the relative location of the second ant with respect to the first one is $(\Delta x, \Delta y) = (2, 3)$, the two ants returns to their initial position after 478 iterations of the rule (provided they started in an uniformly white substrate, with the same direction of motion). A very complicated periodic behavior is observed when $(\Delta x, \Delta y) = (1, 24)$: the two ant start a chaotic-like motion for several thousands of steps. Then, one ant builds a highway and escape from the central region. After a while, the second ant finds the entrance of the highway and rapidly catches the first one. After the two ants meet, they start undoing

their previous paths and return to their original position. This complete cycle takes about 30000 iterations.

More generally, it is found empirically that, when $\Delta x + \Delta y$ is odd and the ants enter their site with the same initial direction , the two-ant motion is likely to be periodic. However, this is not a rule and the configuration $(\Delta x, \Delta y) = (1, 0)$ yields an unbounded motion, a diamond pattern of increasing diameter which is traveled in the same direction by the two ants.

It turns out that the periodic behavior of a two-ant configuration is not so surprising. The rule we defined is reversible in time, provided that there is never more than one ant at the same site. Time reversal symmetry means that if the direction of motion of all ants are reversed, they will move backward through their own sequence of steps, with an opposite direction of motion. Therefore, if at some point of their motion the two ants cross each other (on a lattice link, not on a site), the first ant will go through the past of the second one, and vice versa. They will return to the initial situation (the two ants being exchanged) and build a new pattern, symmetrical to the first one, due to the inversion of the directions of motion. The whole process then cycles for ever. Periodic trajectories are therefore related to the probability that the two ants will, at a some time, cross each other in a suitable way. The conditions for this to happen are fulfilled when the ants sit on a different sublattice (black or white sites on the checkerboard) and exit two adjacent sites against each other. This explain why a periodic motion is likely to occur when $\Delta x + \Delta y$ is odd.

2.7 Population dynamics

In addition to physical, chemical or biological systems, the CA approach is interesting for the study of simple population models. Several different problems can be envisaged, such as the simulation of ecosystems or the social behavior in a population of interacting individuals. Here we consider an example of the latter situation.

The social behavior of the group of persons is certainly related to the fact that each individual has its own autonomy and perception of the environment. On the other hand, the behavior of a whole population may also reflect some "mechanical" or spontaneous response of an individual to the situation it is confronted with. We may hope that the collective behavior that may emerge from such a proceess could be captured by some CA model, provided that one is able to find the rule to which each individual obey. At least it is worth to check whether a given social behavior can be explained with such mechanisms before incriminating the fact that each individual is free to think and act its own way.

Here we address here the generic problem of the competing fight between two different groups over a fixed area. We present a "voter model" which describes the dynamical behavior of a population with bimodal conflicting interests and study the conditions of extinction of one of the initial groups [49].

This model can be thought of as describing the smoker - non smoker fight: in a small group of persons, a majority of smokers will usually convince the few others to smoke and vice versa. The point is really when an equal number of smokers and non-smokers meet. In that case, it may be assumed that a social trend will decide between the two attitudes. In the US, smoking is viewed as a disadvantage whereas, in France, it is rather well accepted. In other words, there is a bias that will select the winner party in an even situation. In our example, whether one studies the French or US case, the bias will be in favor of the smokers or the non-smokers, respectively.

The same mechanism can be associated with the problem of competing standards. The choice of one or the other standard is often driven by the opinion of the majority of people one meets. But, when the two competing systems are equally represented, the intrinsic quality of the product will be decisive. Price and technological advance then play the role of a bias.

Here we consider the case of four-person confrontations in a spatially extended system in which the actors (species A or B) move randomly. Initially, the B species is present with density b_0 and the A species with density $1 - b_0$. The B individuals are supposed to have a qualitative advantage over the As but are less numerous. The question we want to address is what is the minimal density b_0 which make the Bs win over A (i.e. invade the entire system at the expense of A individuals). The process of spatial contamination of opinion plays a crucial role in this dynamics.

The CA rule we propose here [49] to describe this proceess is derived from a model by Galam [50], in which the four individuals involved in a tournament are randomy chosen among the current population, whose composition in A or B type of persons evolves after each confrontation. The density threshold for an invading emergence of B is $b_c = 0.23$ if the B group has a qualitative bias over A. With a spatial distribution of the species, even if $b_0 < b_c$, B can still win over A provided that it strives for confrontation. Therefore a qualitative advantage is found not to be enough to win. A geographic as well a definite degree of aggressiveness are instrumental to overcome the less fitted majority.

The model we use to describe the two populations A and B influencing each other or competing for some unique resources, is based on the diffusion automaton proposed in section 2.5. The particles have two possible internal states (± 1), coding for the A or B species, respectively.

The individuals move on a two-dimensional square lattice. At each site, there are always four individuals (any combination of A's and B's is possible). These four individuals all travels in a different lattice direction (north, east, south and west).

The interaction takes place in the form of "fights" between the four individuals meeting on the same site. At each fight, the group nature (A or B) is updated according to the majority rule, when possible, otherwise with a bias in favor of the best fitted group:

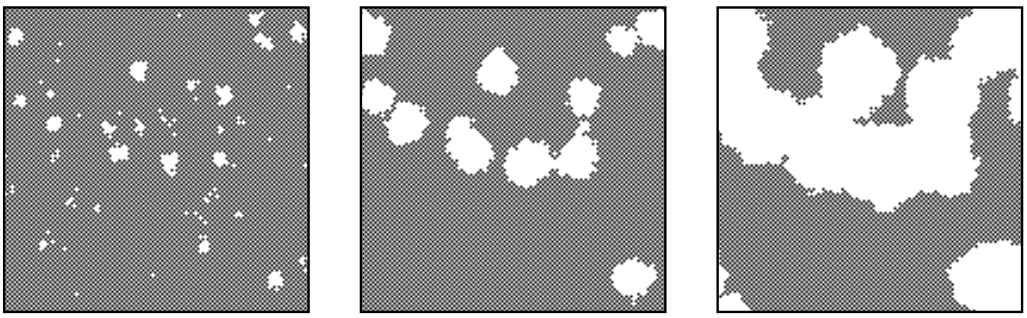

Figure 20: *Configurations of the voter CA model, at three different times. The A and B species are represented by the gray and white regions, respectively. The parameters of the simulation are* $b_0 = 0.1$, $k = 0.5$ *and* $\beta = 1$.

- The local majority species (if any) wins:

$$nA + mB \rightarrow \begin{cases} (n+m)A & \text{if } n > m \\ (n+m)B & \text{if } n < m \end{cases}$$

  where $n + m = 4$.

- When there is an equal number of A and B on a site, B wins the confrontation with probability $1/2 + \beta/2$. The quantity $\beta \in [0, 1]$ is the bias accounting for some advantage (or extra fitness) of species B.

The above rule is applied with probability k. Thus, with probability $1 - k$ the group composition does not change because no fight occurs. Between fights both population agents perform a random walk on the lattice.

The behavior of this model is illustrated in figure 20. The current configuration is shown at three different time steps. We can observe the growth of dense clusters of B invading the system.

It is clear that the model richness comes from the even confrontations. If only odd fights would happen, the initial majority population would always win after some short time. The key parameters of this model are (i) k, the aggressiveness (probability of confrontation), (ii) β, the B's bias of winning a tie and (iii) b_0, the initial density of B.

The strategy according to which a minority of B's (with yet a technical, genetic, persuasive advantage) can win against a large population of A's is not obvious. Should they fight very often, try to spread or accept a peace agreement? We study the parameter space by running the cellular automaton.

In the limit of low aggressiveness ($k \to 0$), the particles move a long time before fighting. Due to the diffusive motion, correlation between successive fights are destroyed and B wins provided that $b_0 > 0.23$ and $\beta = 1$. This is the mean-field

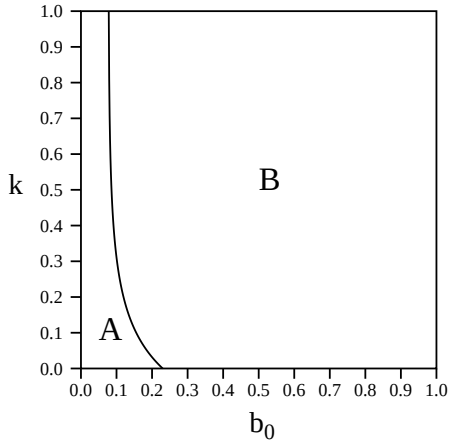

Figure 21: *Phase diagram for our socio-physical model with $\beta = 1$. The curve delineates the regions where, on the left, A wins with high probability and, on the right, B wins with probability one. The outcome depends on b_0, the initial density of B and k, the probability of a confrontation.*

level of our dynamical model which corresponds to the theoretical calculations made in [50].

More generally, we observe that B can win even when $b_0 < 0.23$, provided it acts aggressively, i.e. by having a large enough k. Thus, there is a critical density $b_{death}(k) < 0.23$ such that, when $b_0 > b_{death}(k)$, all A are eliminated in the final outcome. Below b_{death}, B looses unless some specific spatial configurations of B's are present.

Therefore the growth of species B at the expense of A is obtained by a spatial organization. Small clusters that may accidentally form act as nucleus from which the B's can develop. In other words, above the mean-field threshold $b_c = 0.23$ there is no need to organize in order to win but, below this value only condensed regions will be able to grow. When k is too small, such an organization is not possible (it is destroyed by diffusion) and the strength advantage of B does not lead to success.

Figure 21 summarizes, as a function of b_0 and k, the regions where either A or B succeeds. It is found that the separation curve satisfies the equation $(k+1)^7(b_0 - 0.077) = 0.153$.

It is also interesting to study the time needed to annihilate completely the looser. Here, time is measured as the number of fights per site (i.e. kt where t is the iteration time of the automaton). We observe that the dynamics is quite fast and a few units of time are sufficient to yield a collective change of opinion.

Following the same methodology, more complicated interactions between individuals can be investigated. The case of a non-constant bias is quite interesting and is described in [49]. In conclusion, although this model is very simple, it

abstracts the complicated behavior of real life agents by capturing some essential ingredients. For this reason, the results we have presented may shed light on the generic mechanisms observed in a social system of opinion making.

In particular we see that the correlations existing between successive fights may strongly affect the global behavior of the system and that an organization is the key feature to obtain a definite advantage over the other population. This observation is important. For instance, during a campaign against smoking or an attempt to impose a new system, it is much more efficient (and cheaper) to target the effort on small nuclei of persons rather than sending the information in an uncorrelated manner.

2.8 Reactive systems

Diffusive phenomena and reaction processes play an important role in many areas of physics, chemistry and biology and still constitute an active field of research. Systems in which reactive particles are brought into contact by a diffusion process and transform, often give rise to very complex behaviors. Pattern formation [51,52], is a typical example of such a behavior in reaction-diffusion processes.

In addition to a clear academic interest, reaction-diffusion phenomena are also quite important in technical sciences and still constitute numerical challenges. As an example, we may mention the famous problem of carbonation in concrete [53,54].

In many reaction-diffusion problems a particle based model, such as a lattice gas dynamics, provides a useful approach and efficient numerical tool.

For instance, processes such as aggregation, formation of a diffusion front, trapping of particles performing a random walk in some specific region of space [55,56], or the adsorption of diffusing particles on a substrate [57] are important problems that are difficult to solve with the standard diffusion equation. A microscopic model, based on a cellular automata dynamics, is therefore of clear interest.

Reaction processes, as well as growth mechanisms are most of the time nonlinear phenomena, characterized by a threshold dynamics. While they are naturally implemented in terms of a point-particles description they may be very difficult to analyze theoretically and even numerically, with standard techniques, due to the important role that fluctuations may play. In the simplest cases, fluctations are responsible for symmetries breaking which may produce interseting patterns, as we shall see later in this section.

More surprisingly, microscopic fluctuations are sometime relevant at a macroscopic level of observation because they may induce an anomalous dynamics, as in the $A + A \to 0$ or $A + B \to 0$ annihilation reactions [24,58]. These systems depart from the behavior predicted by the classical approach based on differential equations for the densities. The reason is that they are fluctuations-driven and that correlations cannot be neglected. In other words, one has to deal with a full N-body problem and the Boltzmann factorization assumption is not valid.

For this kind of problem, a lattice gas automata approach turns out to be a very successful approach.

Cellular automata particles can be equipped with diffusive and reactive properties, in order to mimic real experiments and model several complex reaction-diffusion-growth processes, in the same spirit as a cellular automata fluid simulates a fluid flow: these systems are expected to retain the relevant aspects of the microscopic world they are modeling. Diffusion can be obtained with the rule described in section 2.5. Chemical reactions, such as $A + B \rightarrow C$, are treated in an abstract way, as a particle transformation phenomena rather than a real chemical interaction (see [3] for more details).

Within the CA approach, there are two ways of modeling a spatially extended system with local reactive interactions. The first one is to use a standard CA scheme: each cell is updated according to the state of its neighbors. The second way is to consider a lattice gas (LG) approach, such as, for instance the HPP dynamics described in section 2.4. LG are a particular class of cellular automata, characterized by a two-phase dynamics: first, a completely local interaction on each lattice point, and then particle transport (or propagation) to nearest-neighbor sites. This way of partitioning the space prevents the problem of having a particle simultaneously involved in several different interactions.

Here we shall consider the first kind of model in which no diffusion is included. The LG paradigm, leading to the usual reaction-diffusion equations is described in detail in [3].

Some reactive phenomena can be nicely described by simple rules. This is the case of several excitable media in which chemical waves are observed and that are now discussed in more detail.

An excitable medium is basically characterized by three states [26]: the resting state, the excited state and the refractory state. The resting state is a stable state of the system. But a resting state can respond to a local perturbation and become excited. Then, the excited state evolves to a refractory state where it no longer influences its neighbors and, finally, returns to the resting state.

A generic behavior of excitable media is to produce chemical waves of various geometries [59,60]. Ring and spiral waves are a typical pattern of excitations. Many chemical systems exhibits an excitable behavior. The Selkov model [61] and the Belousov–Zhabotinsky reaction are examples. Chemical waves play an important role in many biological processes (nervous systems, muscles) since they can mediate the transport of information from one place to another.

The Greenberg–Hasting model is an example of a cellular automata model of an excitable media. This rule, and its generalization, have been extensively studied [62,63].

The implementation we propose here for the Greenberg–Hasting model is the following: the state $\phi(\vec{r}, t)$ of site $\vec{r}$ at time t takes its value in the set $\{0, 1, 2, ..., n-1\}$. The state $\phi = 0$ is the resting state. The states $\phi = 1, ..., n/2$ (n is assumed to be even) correspond to excited states. The rest, $\phi = n/2 + 1, ..., n - 1$ are the

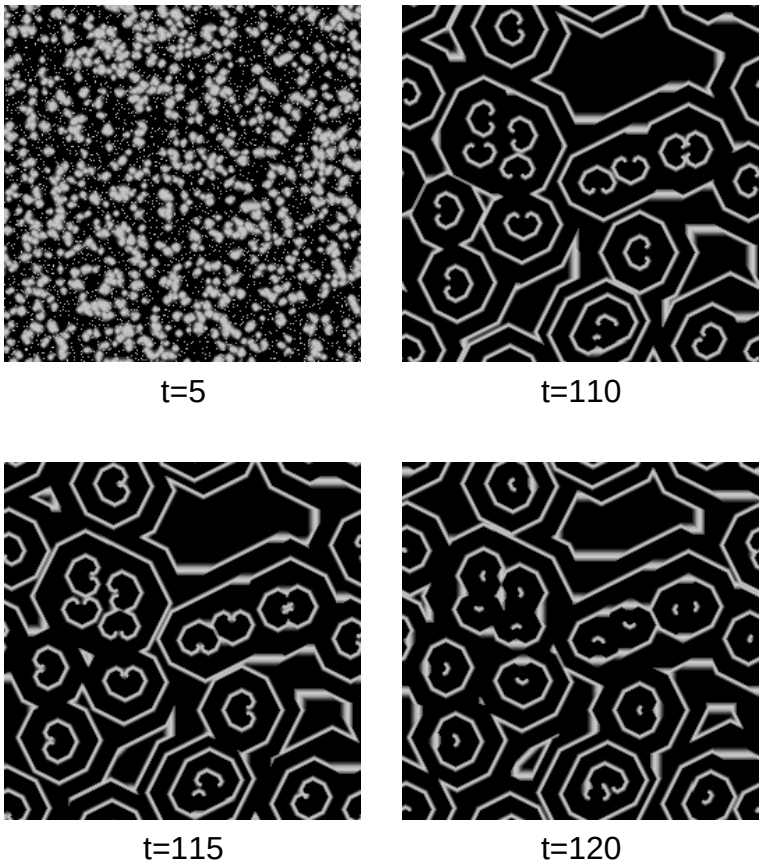

Figure 22: *Excitable medium: evolution of a stable initial configuration with 10% of excited states $\phi = 1$, for $n = 10$ and $k = 3$. The color black indicates resting states. After a transient phase, the system sets up in a state where pairs of counter-rotating spiral waves propagate. When the two extremities come into contact, a new, similar pattern is produced.*

refractory states. The cellular automata evolution rule is the following:

1. If $\phi(\vec{r}, t)$ is excited or refractory, then $\phi(\vec{r}, t+1) = \phi(\vec{r}, t) + 1 \bmod n$.
2. If $\phi(\vec{r}, t) = 0$ (resting state) it remains so, unless there are at least k excited sites in the Moore neighborhood of site $\vec{r}$. In this case $\phi(\vec{r}, t) = 1$.

The n states play the role of a clock: an excited state evolves through the sequence of all possible states until it returns to 0, which corresponds to a stable situation.

The behavior of this rule is quite sensitive to the value of n and the excitation threshold k. Figures 22 and 23 show the evolution of this automaton for two different sets of parameters n and k. Both simulations are started with a uniform configuration of resting states, perturbed by some excited sites randomly distributed over the system. If the concentration of perturbation is low enough,

excitation dies out rapidly and the system returns to the rest state. Increasing the number of perturbed states leads to the formation of traveling waves and self-sustained oscillations may appear in the form of ring or spiral waves.

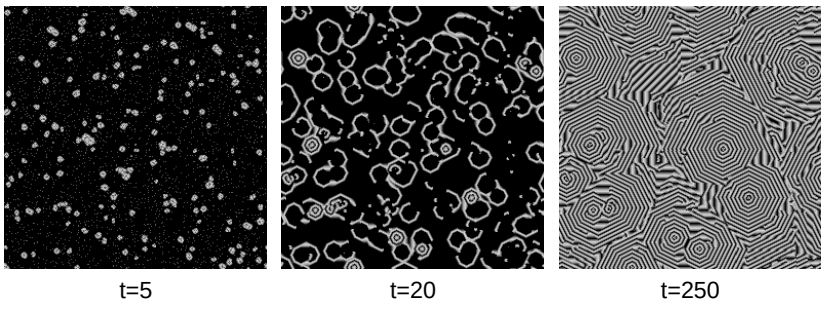

Figure 23: *Excitable medium: evolution of a configuration with 5% of excited states $\phi = 1$, and 95% of resting states (black), for $n = 8$ and $k = 3$.*

The Greenberg–Hasting model has some similarity with the "tube-worms" rule proposed by Toffoli and Margolus [1]. This rule is intended to model the Belousov–Zhabotinsky reaction and is as follows. The state of each site is either 0 (refractory) or 1 (excited) and a local timer (whose value is 3, 2, 1 or 0) controls the refractory period. Each iteration of the rule can be expressed by the following sequence of operations: (i) where the timer is zero, the state is excited; (ii) the timer is decreased by 1 unless it is 0; (iii) a site becomes refractory whenever the timer is equal to 2; (iv) the timer is reset to 3 for the excited sites which have two, or more than four, excited sites in their Moore neighborhood.

Figure 24 shows a simulation of this automaton, starting from a random initial configuration of the timers and the excited states. We observe the formation of spiral pairs of excitations. Note that this rule is very sensitive to small modifications (in particular to the order of operations (i) to (iv)).

Another rule which is also similar to Greenberg-Hasting and Margolus-Toffoli tube-worm models is the so-called forest-fire model. This rule describes the propagation of a fire or, in a different context, may also be used to mimic contagion in case of an epidemic. Here we describe the case of a forest-fire rule.

The forest-fire rule is a probabilitic CA defined on a d-dimensional hypercubic lattice. Initially, each site is occupied by either a tree, a burning tree or is empty. The state of the system is parallel updated according to the following rule: (1) a burning tree becomes an empty site; (2) a green tree becomes a burning tree if at least one of its nearest neighbors is burning; (3) at an empty site, a tree grows with probability p; (4) A tree without a burning nearest neighbor becomes a burning tree during one time step with probability f (lightning).

Figure 25 illustrates the behavior of this rule, in a two-dimensional situation. Provided that the time scales of tree growth and burning down of forest clusters are well separated (i.e. in the limit $f/p \to 0$), this models has self-organized

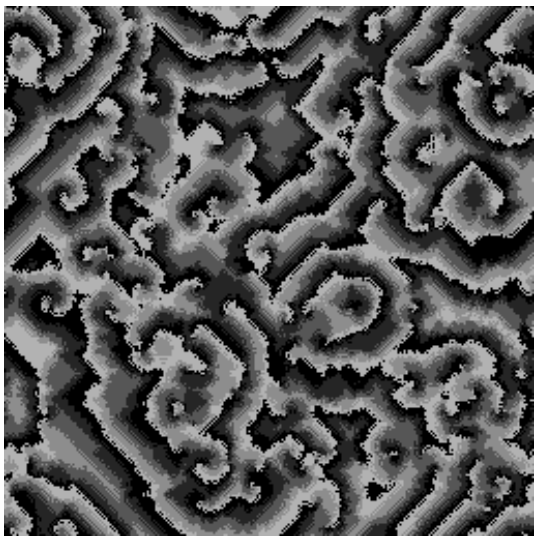

Figure 24: *The tube-worms rule for an excitable media*

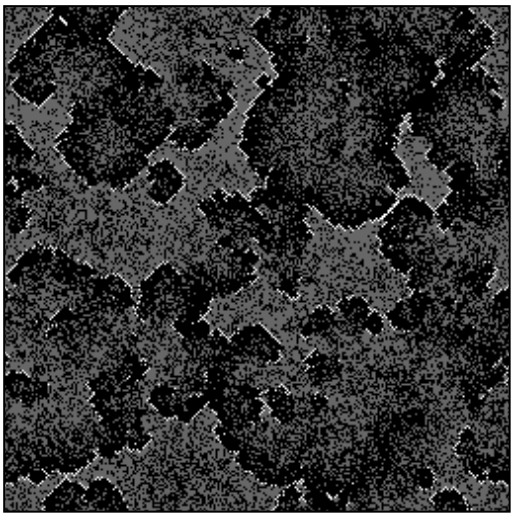

Figure 25: *The forest fire rule: grey sites correspond to a grown tree, black pixels represent burned sites and the white color indicates a burning tree. The snapshot given here represents the situation after a few hundred iterations. The parameters of the rule are* $p = 0.3$ *and* $f = 6 \times 10^{-5}$.

critical states [64]. This means that in the steady state, several physical quantities characterizing the system have a power law behavior. For example, the cluster size distribution $\mathcal{N}(s)$ and radius of a forest cluster $\mathcal{R}(s)$ vary with the number of trees s in the forest cluster as $\mathcal{N}(s) \sim s^{-\tau}\mathcal{C}(s/s_{max})$ and $\mathcal{R}(s) \sim s^{1/\mu}\mathcal{S}(s/s_{max})$ Scaling relations can be established between the critical exponents τ and μ, and the scaling functions $\mathcal{C}$ and $\mathcal{S}$ can be computed.

References

[1] T. Toffoli and N. Margolus. *Cellular Automata Machines: a New Environment for Modeling.* The MIT Press, 1987.

[2] S. Wolfram. *Cellular Automata and Complexity.* Addison-Wesley, Reading MA, 1994.

[3] B. Chopard and M. Droz. *Cellular Automata Modeling of Physical Systems.* Cambridge University Press, 1998.

[4] M. Sipper. *Evolution of Parallel Cellular Machines: The cellular programming approach.* Springer-Verlag, Berlin, 1997. Lecture notes in computer science, vol 1194.

[5] A.W. Burks. Von neumann's self-reproducing automata. In A.W. Burks, editor, *Essays on Cellular Automata*, pages 3–64. University of Illinois Press, 1970.

[6] S. Ulam. Random processes and transformations. *Proc. Int. Congr. Math.*, 2:264–275, 1952.

[7] A. Reggia, S.L. Armentrout, H.-H. Chou, and Y. Peng. Simple systems that exhibit self-directed replication. *Science*, 259:1282, 1993.

[8] D. Mange and M. Tomassini, editors. *Bio-Inspired Computing Machines: towards novel computational architectures.* Press Polytechniques et Universitaires Romandes, 1998.

[9] M. Gardner. The fantastic combinations of john conway's new solitaire game life. *Scientific American*, 220(4):120, 1970.

[10] S. Wolfram. *Theory and Application of Cellular Automata.* World Scientific, 1986.

[11] U. Frisch, B. Hasslacher, and Y. Pomeau. Lattice-gas automata for the navier-stokes equation. *Phys. Rev. Lett.*, 56:1505, 1986.

[12] S. Chen, K. Diemer, G.D. Doolen, K. Eggert, C. Fu, S. Gutman, and B.J. Travis. Lattice gas automata for flow through porous media. *Physica D*, 47:72–84, 1991.

[13] E. Aharonov and D. Rothman. Non-newtonian flow (through porous media): a lattice boltzmann method. *Geophys. Res. Lett.*, 20:679–682, 1993.

[14] D.W. Grunau, T. Lookman, S.Y. Chen, and A.S. Lapedes. Domain growth, wetting and scaling in porous media. *Phys. Rev. Lett.*, 71:4198–4201, 1993.

[15] D.H. Rothman. Immiscible lattice gases:new results, new models. In P. Manneville, N. Boccara, G.Y. Vichniac, and R. Bideau, editors, *Cellular Automata and Modeling of Complex Physical Systems*, pages 206–231. Springer Verlag, 1989. Proceedings in Physics 46.

[16] M. Bonetti, A. Noullez, and J.-P. Boon. Lattice gas simulation of 2-d viscous fingering. In P. Manneville, N. Boccara, G.Y. Vichniac, and R. Bideau, editors, *Cellular Automata and Modeling of Complex Physical Systems*, pages 239–241. Springer Verlag, 1989. Proceedings in Physics 46.

[17] A.K. Gunstensen, D.H. Rothman, S. Zaleski, and G. Zanetti. Lattice boltzmann model of immiscible fluids. *Phys. Rev. A*, 43:4320–4327, 1991.

[18] D. Grunau, Shiyi Chen, and K. Eggert. A lattice boltzmann model for multi-phase fluid flows. *Phys. Fluids A*, 5:2557–2562, 1993.

[19] U. D'Ortona, M. Cieplak, R.B. Rybka, and J.R. Banavar. Two-color nonlinear cellular automata: surface tension and wetting. *Phys. Rev. E*, 51:3718–28, 1995.

[20] A. Károlyi and J. Kertész. Hydrodynamics cellular automata for granular media. In R. Gruber and M. Tomassini, editors, *Proceeding of the 6th Joint EPS-APS International Conference on Physics Computing: PC '94*, pages 675–681, 1994.

[21] G. Peng and H.J. Herrmann. Density waves of granular flow in a pipe using lattice-gas automata. *Phys. Rev. E*, 49:R1796–R1799, 1994.

[22] B. Boghosian, P. Coveney, and A. Emerton. A lattice-gas model of microemulsions. *Proceedings of the Royal Society of London*, 452:1221–1250, 1996.

[23] J.T. Wells, D.R. Janecky, and B.J. Travis. A lattice gas automata model for heterogeneous chemical reaction at mineral surfaces and in pores network. *Physica D*, 47:115–123, 1991.

[24] S. Cornell, M. Droz, and B. Chopard. Some properties of the diffusion-limited reaction $nA+mB \to C$ with homogeneous and inhomogeneous initial conditions. *Physica A*, 188:322–336, 1992.

[25] B. Chopard, P. Luthi, and M. Droz. Reaction-diffusion cellular automata model for the formation of Liesegang patterns. *Phys. Rev. Lett.*, 72(9):1384–1387, 1994.

[26] J.-P. Boon, D. Dab, R. Kapral, and A. Lawniczak. Lattice gas automata for reactive systems. *Phys. Rep.*, 273:55–148, 1996.

[27] D.E. Wolf, M. Schreckenberg, and A. Bachem, editors. *Traffic and Granular Flow*. World Scientific, 1996.

[28] D.E. Wolf and collaborator, editors. *Traffic and Granular Flow '97*. Springer, to appear.

[29] B. Chopard, P. O. Luthi, and P.-A. Queloz. Cellular automata model of car traffic in two-dimensional street networks. *J. Phys. A*, 29:2325–2336, 1996.

[30] E. Banks. Information processing and transmission in cellular automata. Technical report, MIT, 1971. MAC TR-81.

[31] G.G. McNamara and G. Zanetti. Use of the boltzmann equation to simulate lattice-gas automata. *Phys. Rev. Lett.*, 61:2332–2335, 1988.

[32] F. Higuera, J. Jimenez, and S. Succi. Boltzmann approach to lattice gas simulations. *Europhys. Lett*, 9:663, 1989.

[33] D.B. Bahr and J.B. Rundle. Theory of lattice boltzmann simulation of glacier flow. *J. of Glaciology*, 41(139):634–40, 1995.

[34] G. Vichniac. Simulating physics with cellular automata. *Physica D*, 10:96–115, 1984.

[35] J.D. Gunton and M. Droz. *Introduction to the Theory of Metastable and Unstable States*. Springer Verlag, 1983.

[36] Pascal O. Luthi, Anette Preiss, Jeremy J. Ramsden, and B. Chopard. A cellular automaton model for neurogenesis in drosophila. *Physica D*, 118:151–16–, 1998.

[37] S. Yukawa, M. Kikuchi, and S. Tadaki. Dynamical phase transition in one-dimensional traffic flow model with blockage. *J. Phys. Soc. Jpn*, 63(10):3609–3618, 1994.

[38] M. Schreckenberg, A. Schadschneider, K. Nagel, and N. Ito. Discrete stochastic models for traffic flow. *Phys. Rev. E*, 51:2939, 1995.

[39] A. Schadschneider and M. Schreckenberg. Cellular automaton models and traffic flow. *J. Phys.*, A(26):L679, 1993.

[40] K. Nagel and M. Schreckenberg. Cellular automaton model for freeway traffic. *J. Physique I (Paris)*, 2:2221, 1992.

[41] K. Nagel and H.J. Herrmann. Deterministic models for traffic jams. *Physica A*, 199:254, 1993.

[42] A. Dupuis. Simulateur micro-cellulaire parallèle de trafic routier urbain et application à la ville de Genève. Technical report, CUI, University of Genev, 1997. Master disertation.

[43] B. Chopard, A. Dupuis, and P. Luthi. A cellular automata model for urban traffic and its application to the city of geneva. In M. Schreckenberg and D.E. Wolf, editors, *Traffic and Granular Flow '97*, pages 153–168. Springer-Verlag, Singapore, 1998.

[44] T. Vicsek. *Fractal Growth Phenomena*. World Scientific, 1989.

[45] T.A. Witten and L.M. Sander. Diffusion-limited aggregation. *Phys. Rev. B*, 27:5686, 1983.

[46] S. Tolman and P. Meakin. Off-lattice and hypercubic-lattice models for diffusion-limited aggregation in dimension 2–8. *Phys. Rev. A*, 40:428–37, 1989.

[47] I. Stewart. The ultimate in anty-particle. *Scientific American*, pages 88–91, July 1994.

[48] J. Propp. Trajectory of generalized ants. *Math. Intelligencer*, 16(1):37–42, 1994.

[49] S. Galam, B. Chopard, A. Masselot, and M. Droz. Competing species dynamics: Qualitative advantage versus geography. *Eur. Phys. J. B*, 4:529–531, 1998.

[50] Serge Galam. Social paradoxes of majority rule voting and renormalization group. *J. Stat. Phys.*, 61:943–951, 1990.

[51] J. E. Pearson. Complex patterns in a simple system. *Science*, 261:189–192, July 1993.

[52] J.D. Muray. *Mathematical Biology*. Springer-Verlag, 1990.

[53] L.M. Brieger and E. Bonomi. A stochastic cellular automaton model of nonlinear diffusion and diffusion with reaction. *J. Comp. Phys.*, 94:467–486, 1991.

[54] E.J. Garboczi. Permeability, diffusivity and microstructural parameters: a critical review. *Cement and Concrete Res.*, 20:591–601, 1990.

[55] G.H. Weiss. Random walks and their applications. *American Scientist*, 71:65, 1983.

[56] G.H. Weiss, editor. *Contemporary Problems in Statistical Physics*. SIAM, 1994.

[57] P. O. Luthi, J. Ramsden, and B. Chopard. The role of diffusion in irreversible deposition. *Phys. Rev. E*, 55:3111–3115, 1997.

[58] S. Cornell, M. Droz, and B. Chopard. Role of fluctuations for inhomogeneous reaction-diffusion phenomena. *Phys. Rev. A*, 44:4826–32, 1991.

[59] R. Kapral and K. Showalter, editors. *Chemical Waves and Patterns*. Kluwer Academic, 1995.

[60] J.P. Keener and J.J. Tyson. The dynamics of scroll waves in excitable media. *SIAM Rev.*, 34:1–39, 1992.

[61] E.E. Selkov. Self-oscillation in glycolysis: A simple kinetic model. *Eur. J. Biochem.*, 4:79, 1968.

[62] R. Fisch, J. Gravner, and D. Griffeath. Threshold-range scaling of excitable cellular automata. *Statistics and Computing*, 1:23, 1991.

[63] J. Gravner and D. Griffeath. Threshold grouse dynamics. *Trans. Amer. Math. Soc.*, 340:837, 1993.

[64] B. Drossel and F. Schwabl. Self-organized critical forest-fire model. *Phys. Rev. Lett.*, 69:1629, 1992.